



You have downloaded a document from
RE-BUS
repository of the University of Silesia in Katowice

Title: Preparation and magnetic characteristics of $\text{Co}_{1-\delta}\text{Zn}_\delta\text{Fe}_2\text{O}_4$ ferrite nanopowders

Author: Marian Kubisztal, I. Herok, Małgorzata Karolus, Krystian Prusik, Grzegorz Haneczok

Citation style: Kubisztal Marian, Herok I., Karolus Małgorzata, Prusik Krystian, Haneczok Grzegorz. (2017). Preparation and magnetic characteristics of $\text{Co}_{1-\delta}\text{Zn}_\delta\text{Fe}_2\text{O}_4$ ferrite nanopowders. "Acta Physica Polonica. A" (Vol. 131, nr 5 (2017), s. 1236-1239), doi 10.12693/APhysPolA.131.1236



Uznanie autorstwa - Użycie niekomercyjne - Bez utworów zależnych Polska - Licencja ta zezwala na rozpowszechnianie, przedstawianie i wykonywanie utworu jedynie w celach niekomercyjnych oraz pod warunkiem zachowania go w oryginalnej postaci (nie tworzenia utworów zależnych).



UNIwersYTET ŚLĄSKI
W KATOWICACH



Biblioteka
Uniwersytetu Śląskiego



Ministerstwo Nauki
i Szkolnictwa Wyższego

Preparation and Magnetic Characteristics of $\text{Co}_{1-\delta}\text{Zn}_\delta\text{Fe}_2\text{O}_4$ Ferrite Nanopowders

M. KUBISZTAL*, I. HEROK, M. KAROLUS, K. PRUSIK AND G. HANECZOK

Institute of Materials Science, University of Silesia, 75 Pułku Piechoty 1A, 41-500 Chorzów, Poland

In the present paper the $\text{Co}_{1-\delta}\text{Zn}_\delta\text{Fe}_2\text{O}_4$ ($0 \leq \delta \leq 1$) ferrite nanopowders with a spinel type structure were synthesized using a chemical co-precipitation technique with constant flow rate $\nu_{FR} = 120 \text{ cm}^3/\text{min}$ at three different reaction temperatures i.e. $T_r = 50^\circ\text{C}$, 70°C and 90°C . Magnetic and structural characteristics of the obtained materials were investigated by means of X-ray diffraction method, transmission electron microscopy and vibrating sample magnetometer. In the course of studies hysteresis loops $M(\mu_0 H)$ and the relations of magnetization M_{7T} (determined at $\mu_0 H = 7 \text{ T}$), squareness ratio S and the Néel temperature T_N versus Zn content were determined and discussed in detail. It was shown that for $\delta < 0.6$ the increase in reaction temperature T_r results in a significant increase of the measured magnetic characteristics. In particular, in the case of $\text{Co}_{0.8}\text{Zn}_{0.2}\text{Fe}_2\text{O}_4$ ferrite nanopowder magnetization M_{7T} reaches maximal value of about 80 emu/g .

DOI: [10.12693/APhysPolA.131.1236](https://doi.org/10.12693/APhysPolA.131.1236)

PACS/topics: 75.47.Lx, 75.50.Gg, 75.50.Tt, 75.75.-c, 75.75.Cd

1. Introduction

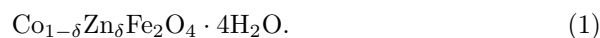
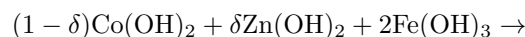
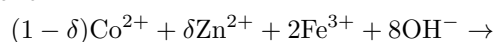
Magnetic nanoparticles are of significant interest in fundamental research and have found already many industrial applications. One can mention their high catalytic activity and applications in drug delivery systems or in MRI technology as contrasts agents [1–4]. Especially interesting are magnetic oxide nanoparticles with a spinel type structure and chemical composition of the form MFe_2O_4 where M denotes Co, Zn, Mn, Cu etc. In this kind of material (called ferro-spinel nanoparticles) the oxide ions O^{2-} create fcc structure (mainly $Fd\bar{3}m$ space group) with 8 tetrahedral and 16 octahedral sites occupied by divalent M^{2+} and trivalent Fe^{3+} ions. Important is that different occupation of two sublattices by ferromagnetic additions may cause a compensation of magnetism and in consequence allows one to obtain unique properties of the ferro-spinel nanoparticles. In addition, a distortion of a magnetic structure occurring at a nanoparticle surface and magnetic interactions between neighboring nanoparticles may also significantly change functional characteristics of the final material [5–13].

In this context, it is proper to add that some properties of the ferrite nanoparticles can be controlled by technological parameters applied in the production process. In our work we have synthesized the $\text{Co}_{1-\delta}\text{Zn}_\delta\text{Fe}_2\text{O}_4$ nanopowder with $0 \leq \delta \leq 1$ by applying standard wet chemical technique based on co-precipitation of nanoparticles in water solutions [14, 15]. Note that from a technological point of view, the control of nanoparticle properties is a difficult problem as in nanoscale properties of fabricated materials strongly depend not only on chemical composition, but also on the size. In this paper, we

have determined such characteristics of cobalt-zinc ferrite nanopowders as: unit cell parameter a_0 , crystallite size D_c , lattice strain ε and particle size D_p . The influence of chemical reaction temperature T_r and chemical composition on basic magnetic properties (i.e. the magnetic parameters of the hysteresis loops, the Néel temperature T_N and the loop squareness S) of synthesized nanopowders has been also determined and discussed in detail. The applied synthesis procedure, experimental techniques and obtained results were presented in next sections.

2. Synthesis and experimental

Co–Zn ferrite nanoparticles with chemical formula $\text{Co}_{1-\delta}\text{Zn}_\delta\text{Fe}_2\text{O}_4$ ($\delta = 0, 0.2, 0.6, \text{ and } 1$) were synthesized using chemical co-precipitation in water solutions. In this approach one can obtain materials with different concentration of Zn by applying the chemical reaction of the form:



The syntheses were carried out at $\text{pH} > 10$ in a helium atmosphere with solutions magnetically stirred at 500 r.p.m. All ingredients were of analytical purity (purchased in POCH Gliwice) and double distilled water with resistivity $182 \text{ k}\Omega\text{m}$ was used. Dependently on the coefficient δ the concentrations of prepared solutions were changed according to the following pattern: $0.2 \text{ mol/dm}^3 \text{ FeCl}_3 \cdot 6\text{H}_2\text{O}$, $x \text{ mol/dm}^3 \text{ CoCl}_2$ and $(0.1 - x) \text{ mol/dm}^3 \text{ ZnCl}_2$ with $0 \leq x \leq 0.1$. In the next step, the prepared chloride solutions were added to $10 \text{ mol/dm}^3 \text{ NaOH}$ — that acts as a precipitating agent — with constant flow rate $\nu_{FR} = 120 \text{ cm}^3/\text{min}$. The amount of Co–Zn ferrite nanopowder produced in one

*corresponding author; e-mail: marian.kubisztal@us.edu.pl

synthesis in all cases was established to 250 mg. Time of chemical reaction was fixed at 2 h and reaction temperature T_r was established as 50 °C, 70 °C and 90 °C. In the last step, the obtained nanoparticles were rinsed in distilled water and ethyl alcohol using decantation and centrifugation at 300 r.p.m., then dried at 50 °C for 48 h and heated in air atmosphere at temperature 700 °C for 1 h (slow cooling).

X-ray diffraction measurements (XRD) were performed using Empyrean PANalytical Diffractometer (Cu K_α radiation). Phase analysis and structure studies (the Rietveld refinements [16]) were carried out by applying High Score Plus PANalytical software integrated with ICDD PDF4+ crystallographic data base. In order to determine the crystallite size D_c and the lattice strain ε the Williamson–Hall method was applied [17]. Additional studies of the obtained nanoparticles were carried out using a high resolution transmission electron microscope JEM 3010. In particular, TEM images allowed one to calculate the size distribution of ferrite nanoparticles by counting the number of particles with a given diameter. However, taking into account high tendency to agglomeration before TEM observations all nanoparticles were coated with oleic acid according to the following procedure: (i) dispersion of ferrite nanopowder in water solution of NaOH (Ph 10.5) and oleic acid, (ii) preliminary deagglomeration in ultrasonic bath for 0.5 h, (iii) magnetic stirring at temperature 90 °C/1 h, (iv) rinsing of nanoparticles in distilled water and acetone and (v) drying at 50 °C/24 h. All magnetic measurements were performed using VSM Quantum Design apparatus operating in temperature range 2–400 K and magnetic field up to 7 T.

3. Results and discussion

Figure 1 presents the results of XRD analysis obtained for $\text{Co}_{1-\delta}\text{Zn}_\delta\text{Fe}_2\text{O}_4$ nanopowder with $\delta = 0, 0.2, 0.6,$ and 1 after thermal treatment at 700 °C/1 h in air atmosphere. It is obvious that independently of δ the obtained nanopowders crystallize in a spinel type structure. Namely, in the case of ZnFe_2O_4 the registered diffraction lines correspond to space group $Fd\bar{3}m$ with unit cell parameter $a_0 = 8.4300$ Å (card number: 00-001-1108 ICDD PDF4). The diffraction lines of CoFe_2O_4 nanopowder, correspond to space group $Fd\bar{3}m$ with unit cell parameter $a_0 = 8.3900$ Å (card number: 00-001-1121 ICDD PDF4). According to that data the lattice constant a_0 of ferrite nanopowder with δ between 0 and 1 should be higher than 8.3900 Å and lower than 8.4300 Å as it is predicted by the Vegard law. Such statement is confirmed by XRD analysis where the lattice parameters corresponding to $\delta = 0.2$ and 0.6 are equal to 8.3915 and 8.4152 Å, respectively (see Table I). It can be also seen that in the case of ZnFe_2O_4 nanopowder the determined value of crystallite size D_c is slightly lower while the lattice strains ε are higher in comparison with the cobalt and cobalt–zinc ferrites.

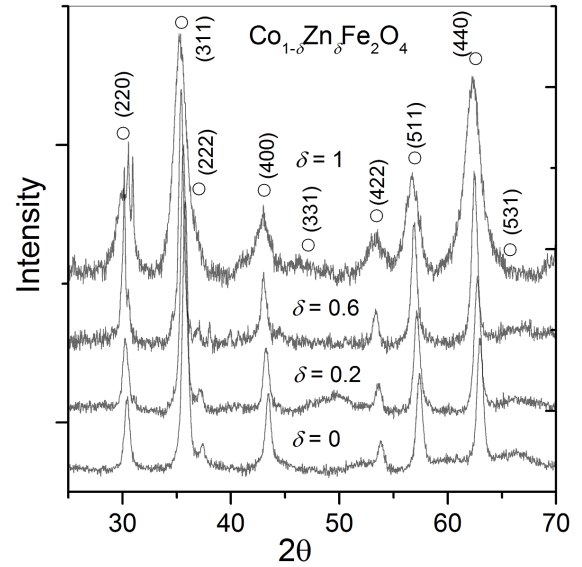


Fig. 1. XRD results obtained for $\text{Co}_{1-\delta}\text{Zn}_\delta\text{Fe}_2\text{O}_4$ ($0 \leq \delta \leq 1$) after thermal treatment at 700 °C/1 h.

TABLE I

Unit cell parameter (a_0), crystallite size (D_c) and lattice strain (ε) obtained for $\text{Co}_{1-\delta}\text{Zn}_\delta\text{Fe}_2\text{O}_4$ after annealing at 700 °C/1 h.

δ	a_0 [Å]	D_c [nm]	ε [%]
0	8.3771	14(1)	0.22
0.2	8.3915	14(1)	0.24
0.6	8.4152	15(1)	0.21
1.0	8.4508	6(1)	0.55

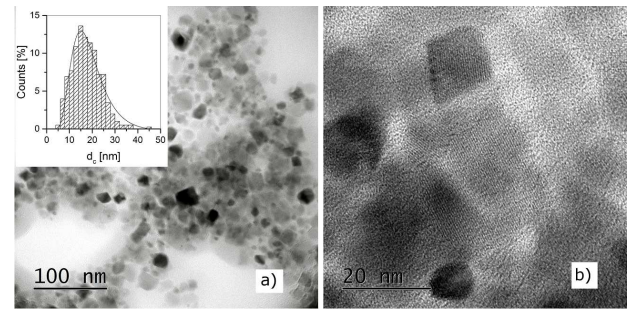


Fig. 2. TEM images of $\text{Co}_{0.4}\text{Zn}_{0.6}\text{Fe}_2\text{O}_4$, ferrite nanopowder obtained at $T_r = 90$ °C and $\nu_{FR} = 120$ cm^3/min : (a) picture in bright field, and (b) in high resolution mode. In the inset histogram of the nanoparticle size.

Figure 2 shows TEM images — in bright field (Fig. 2a) and in high resolution mode (Fig. 2b) obtained for arbitrary selected $\text{Co}_{0.4}\text{Zn}_{0.6}\text{Fe}_2\text{O}_4$ nanopowder synthesized at $T_r = 90$ °C. It can be seen that singular particles are clearly separated by surfactant molecules and some of the particles characterize a rectangular shape with clearly seen edges. In the inset, the histogram of nanoparticle

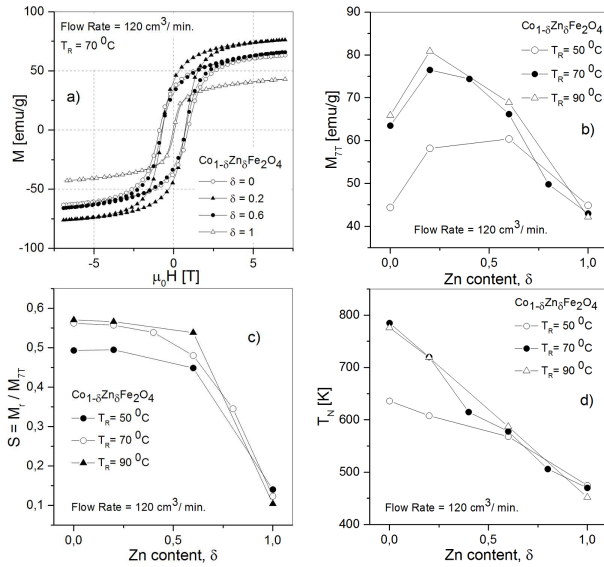


Fig. 3. Magnetic characteristics of $\text{Co}_{1-\delta}\text{Zn}_\delta\text{Fe}_2\text{O}_4$ nanopowders: (a) hysteresis loops $M(\mu_0H)$ (5 K), (b) magnetization $M_{7\text{T}}$ determined in magnetic field $\mu_0H = 7\text{ T}$ (5 K) vs. Zn content δ , (c) squaresness ratio $S = M_r/M_{7\text{T}}$ (5 K) vs. Zn content δ and (d) Néel's temperature T_N vs. Zn content δ ; T_r — chemical reaction temperature.

size with fitted lognormal distribution was also presented. In the studied case, the mean nanoparticle size is equal to 17.6(0.4) nm which is in good agreement with mean crystallites size obtained from XRD measurements i.e. 15(1) nm.

Figure 3a presents hysteresis loops $M = f(\mu_0H)$ determined at temperature 5 K for $\text{Co}_{1-\delta}\text{Zn}_\delta\text{Fe}_2\text{O}_4$ ferrite nanopowders ($\delta = 0, 0.2, 0.6$ and 1) synthesized at $T_r = 70^\circ\text{C}$. It can be seen that the measured hystereses characterize high symmetry with coercive field μ_0H_c ranging from 0.05 T to 0.9 T dependently on Zn content. It can be also seen that even at a high magnetic field (up to 7 T) magnetization in saturation is not reached.

Figure 3b presents the relation of $M_{7\text{T}}$ (i.e. magnetization of the sample measured at magnetic field 7 T) vs. Zn content δ obtained for the ferrite nanopowders synthesized at different reaction temperatures T_r i.e. 50°C , 70°C and 90°C . In that case, for $T_r = 70^\circ\text{C}$ and 90°C we observe a broad peak with maximum located at $\delta = 0.2$ and with the value $M_{7\text{T}}$ of about 80 emu/g. However, for $T_r = 50^\circ\text{C}$ the maximum is shifted to higher values of δ (i.e. 0.6) and reaches significantly lower $M_{7\text{T}}$ i.e. 60 emu/g. Such results suggest that magnetic characteristics of $\text{Co}_{1-\delta}\text{Zn}_\delta\text{Fe}_2\text{O}_4$ ferrite nanopowders may be tailored by a proper placing of Co^{2+} , Zn^{2+} and Fe^{3+} ions in tetrahedral (A) and octahedral (B) sites of the spinel structure.

According to the Néel two-sublattice model of ferromagnetism the resultant magnetic moment μ_r calculated per formula unit (in the Bohr magnetons) is equal to

$\mu_b - \mu_a$, i.e. to the difference between magnetic moments located in octahedral (μ_b) and tetrahedral (μ_a) sites. It means that a partial substitution of Co^{2+} ions by non-magnetic Zn^{2+} ions causes a decrease in μ_a and — in consequence — to initial increase of $M_{7\text{T}}$ observed in Fig. 3b.

However, further incorporation of nonmagnetic Zn^{2+} ions results in a significant decrease of sample magnetization $M_{7\text{T}}$ as it should be expected. Figure 3c shows squaresness S of the hysteresis loops defined as $M_r/M_{7\text{T}}$ (M_r — magnetic remanence) plotted versus Zn content. It can be seen that in this case an increase in δ results in a strong decrease in S which means that addition of non-magnetic Zn^{2+} ions significantly influences also magnetization processes and magnetic moment interactions taking place in the studied materials as the observed change in S reaches even 80%.

Similar correlation can be found in Fig. 3d which presents the relations of the Néel temperature T_N vs. Zn content obtained for the studied Co - Zn ferrite nanopowders. Here, an increase in δ results in a strong decrease in T_N , the observed change is from 780 K ($\delta = 0$) to 465 K ($\delta = 1$). It is obvious that such a decrease is related to a change of long-range ferrimagnetic interactions that gradually diminish with increasing δ . Namely, an increase in Zn^{2+} content in chemical composition of the studied ferrite nanoparticles hinders the exchange interactions between magnetic moments of the ions located in A and B sublattice and leads to the observed changes of such magnetic characteristics as T_N or S . Note also that for $\delta < 0.6$ the measured T_N is significantly lower for nanoparticles obtained at reaction temperature $T_r = 50^\circ\text{C}$. It seems that in this case the magnetism is influenced by distorted structure of the ferrite nanoparticles fabricated at lower temperatures T_r . Taking the above results into consideration one can state that the decrease of reaction temperature T_r from 90°C to 50°C strongly affects magnetic properties of $\text{Co}_{1-\delta}\text{Zn}_\delta\text{Fe}_2\text{O}_4$ ferrite nanopowders with δ lower than 0.6 and there is no significant difference in determined magnetic characteristics of the ferrites obtained at $T_r = 70^\circ\text{C}$ and 90°C .

4. Concluding remarks

In the present paper $\text{Co}_{1-\delta}\text{Zn}_\delta\text{Fe}_2\text{O}_4$ nanopowder with $\delta = 0, 0.2, 0.6$ and 1 were synthesized by applying standard chemical co-precipitation route. Appropriate synthesis was carried out in three different reaction temperatures $T_r = 50^\circ\text{C}$, 70°C , and 90°C with flow-rate parameter $120\text{ cm}^3/\text{min}$. XRD results confirmed that synthesized materials characterize a spinel type structure with crystallites size less than 20 nm and with unit cell parameter a_0 in the range 8.3771–8.4508 Å. It was shown that magnetic and structural characteristics of the ferrite nanoparticles strongly depend on Co^{2+} and Zn^{2+} distribution between two sublattices. In particular, the maximal value of magnetization $M_{7\text{T}}$ determined at magnetic field 7 T and at temperature 5 K was registered for $\text{Co}_{0.8}\text{Zn}_{0.2}\text{Fe}_2\text{O}_4$ nanopowder and it was equal

to 80 emu/g. It was also stated that ferrite nanopowders with $\delta < 0.6$ obtained at reaction temperatures $T_r = 70^\circ\text{C}$ and 90°C show significantly higher magnetic characteristics in comparison with ferrite nanopowders obtained at $T_r = 50^\circ\text{C}$.

References

- [1] N. Sanpo, C.C. Berndt, C. Wen, J. Wang, *Acta Biomater.* **9**, 5830 (2013).
- [2] E. Tombácz, D. Bica, A. Hajdú, E. Illés, A. Majzik, L. Vékás, *J. Phys. Condens. Matter* **20**, 204103 (2008).
- [3] B. Issa, I.M. Obaidat, B.A. Albiss, Y. Haik, *Int. J. Mol. Sci.* **14**, 21266 (2013).
- [4] D.S. Mathew, R.S. Juang, *Chem. Eng. J.* **129**, 51 (2007).
- [5] R.V. Upadhyay, H. Parmar, P. Acharya, A. Banerjee, *Solid State Commun.* **163**, 50 (2013).
- [6] H. Sozeri, Z. Durmus, A. Baykal, *Mater. Res. Bull.* **47**, 2442 (2012).
- [7] A.V. Raut, R.S. Barkule, D.R. Shengule, K.M. Jadhav, *J. Magn. Magn. Mater.* **358**, 87 (2014).
- [8] R.N. Bhowmik, R. Ranganathan, B. Ghosh, S. Kumar, S. Chattopadhyay, *J. Alloy. Comp.* **456**, 348 (2008).
- [9] N.M. Deraz, A. Alarifi, *J. Anal. Appl. Pyrol.* **94**, 41 (2012).
- [10] M. Kubisztal, A. Chrobak, J. Kubisztal, J. Stabik, A. Dybowska, G. Haneczok, *Solid State Phenom.* **203**, 310 (2013).